

## A Photovoltaic Water Pump Testing Facility

**P.K. Koner and J.C. Joshi**

Photovoltaic Laboratory, Centre for Energy Studies  
Indian Institute of Technology, Delhi  
New Delhi 110016, INDIA

**K.L. Chopra**

Director, Indian Institute of Technology, Kharagpur  
Kharagpur 721302, INDIA.

LIBRARY IRC  
PO Box 93190, 2509 AD THE HAGUE  
Tel.: +31 70 30 689 80  
Fax: +31 70 35 899 64

### ABSTRACT

BARCODE: 9149  
LO: 232.4 91PH

*A closed loop and multipurpose photovoltaic water pump testing system has been designed and fabricated. It has been used to carry out a comparative study of the individual and conjugate field performances and system efficiencies (individual components and total) of two motor-pumps. Three power sources can be used to characterize the motor-pumps and to compare the study results of different pump systems. A high wattage current/voltage characteristics meter for solar cells or arrays and a switching device for changing the combinations of PV modules have been designed and developed and these were connected to the testing system. The importance and the field performance of this test system have been discussed by a comparative and individual technical and cost analysis study of two different motor-pump systems. A comparative study of both the systems show the superiority of the DC series motor-pump (C.E.L., India) system under Indian conditions.*

### INTRODUCTION

Photovoltaic (PV) water pumping as an application of PV energy is expected to increase in popularity in the near future. The characteristics of a PV pumping system depend on a number of requirements and environmental parameters. Therefore, before the installation of a PV water pumping system on site, a detailed study of its performance equivalent to outdoor conditions should be made. The manufacturer's specifications are not sufficient to design a system for outdoor conditions because the specified data are generally quoted only for the best results of the system under a particular set of conditions, viz., water head and voltage. The main variables under outdoor conditions are the variation of seasonal ground water depth and change in solar insolation level during a day. For studying the performance of a PV water pump system, a test facility is required. Different types of PV water pump testing systems have been reported in the literature [1-3]. However, these test systems were designed and developed for the study of a particular type of PV water pump system. A modified and versatile closed loop and multipurpose PV water pump testing system has been designed and fabricated and is discussed herein.

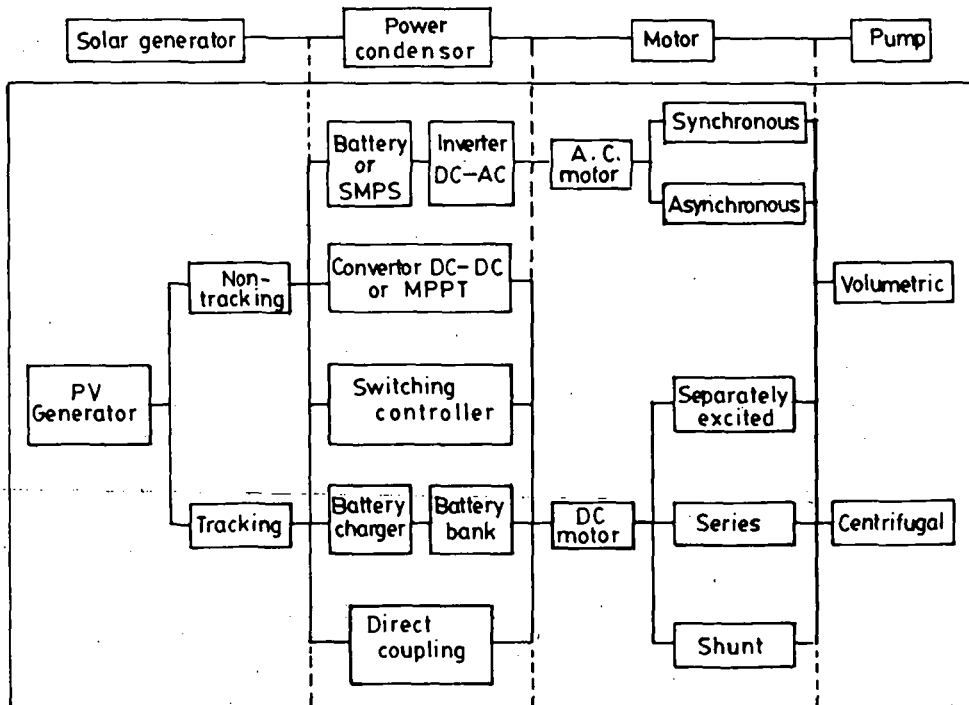
The field performance of the testing system has been verified by a comparative study of two different water pump systems. Individual component and total system studies, operating norms

232.4-91PH-9149

and cost analysis for both the systems have been made with solar insolation and static water head as variables. The average daily efficiency and projected specific capital cost (S.C.C.) have been calculated from the collected field data and compared for both the systems.

## DESCRIPTION OF TESTING FACILITY

The design versatility of PV water pump systems, as shown in Fig.1, necessitates the design and development of a multipurpose PV water pump testing system, and this is shown in Fig. 2. The testing system consists of a 2 kWp PV generator, a 12 kVA battery bank, a 1 kVA DC-AC inverter to produce AC power from a PV generator, a 1 kVA DC-AC power supply to supply constant voltage to the load, a 220 volts AC supply, a 500 watts current/voltage characteristics meter for solar cells and arrays, a 600 watts MPPT and a switching device for changing the combination of PV modules. This system can study the individual and comparative field performances of a number of different water pump systems. Different power sources e.g. battery, DC constant voltage source, PV generator, AC supply are connected to the water pump testing system to compare their performances. The system has three pumps in parallel, separated by valves and flanges, in such a fashion that their individual and conjugate performance can be studied. A globe valve regulating device has been employed in the PV water pump set-up to create back pressure on the pump for the calibration of an equivalent water head. The developed back pressure has been



MPPT - Maximum power point tracker  
SMPS - Switch mode power supply

Fig. 1. Block diagram for the components of a photovoltaic water pump system.

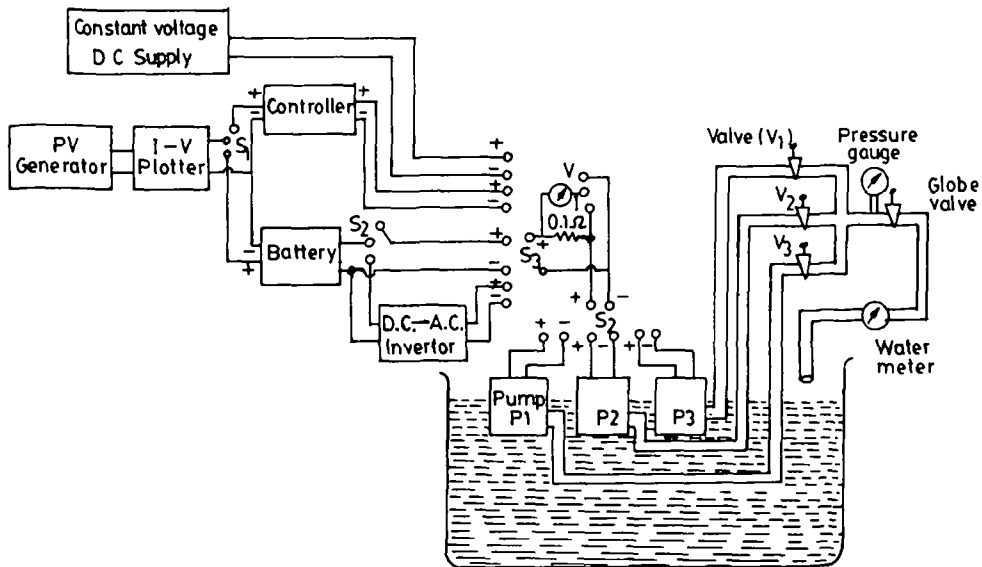


Fig. 2. Experimental set-up of photovoltaic water pump.

Table 1. Specification of C.E.L. cz-Si PV module at STC.

No. of Solar Cells (connected in series)	Area of Each Solar Cell (cm)	$V_{oc}$ (volts)	$I_{sc}$ (amps)	$V_m$ (volts)	$I_m$ (amps)	$P_m$ (watts)
36	78.5	21.0	2.2	16.2	1.98	32.0

measured and calibrated by a pressure gauge where 1 kg/cm<sup>2</sup> is equal to a water head of 10 metres. One water meter is used here for measuring the flow rate and total volume of water for a day. To evaluate the motor constant (M) and torque of the system, speed is an important parameter. The speed of the system has been measured by using a tachometer.

### PV Generator

The PV generator is formed by 70 PV modules which are manufactured by C.E.L., India. The specifications of these modules are shown in Table 1.

The PV generator can be characterized under field conditions by drawing current-voltage curves by a high wattage I-V plotter. Therefore, a high wattage current/voltage characteristics meter is an important component of a PV water pump testing facility. From the I-V curves,  $V_m$ ,  $I_m$ ,  $I_{sc}$  and  $V_{oc}$  of the PV generator are found. The efficiency ( $E_a$ ) of the PV array can be computed by measuring solar insolation as

$$E_a = P_m \times 100 / (SI \times A) \tag{1}$$

To study the performance of the PV generator, a 500 watts current/voltage characteristics meter has been designed and fabricated as shown in Fig. 3. The basic principle of the electronic load current/voltage characteristics meter is described. The resistance of a power transistor is varied from almost zero to infinity by controlling its base current from 0 to  $(I_B)_{max}$  by changing its voltage from 0.7 volt to 0.0 volt. Therefore, the operating point of the PV device is varied from near short circuit to open circuit. Since the collector to emitter saturation voltage of the transistor is 0.7 volt in ON condition, the voltage across the PV device does not reach 0.0 volt corresponding to short circuit. However, this does not affect the  $I_{sc}$  value because the current is nearly constant until the voltage is a few volts.

In this plotter, a galvanometer is used for measuring three parameters, namely: solar insolation, current, and voltage of the solar cells or array by proper switchings. On connecting a reference solar cell (0.036 cm<sup>2</sup>) using S1 directly to the galvanometer (resistance nearly 0.0 ohm), we can obtain the solar insolation in terms of the short circuit current measured. Since maximum galvanometer current limit is 12 mA, this will give us a maximum of 1200 W/m<sup>2</sup> solar insolation, because the short circuit current of the reference solar cell is 12 mA at a solar insolation of 1200 W/m<sup>2</sup>. For I-V measurement of a PV device, the galvanometer is used as a voltmeter. The

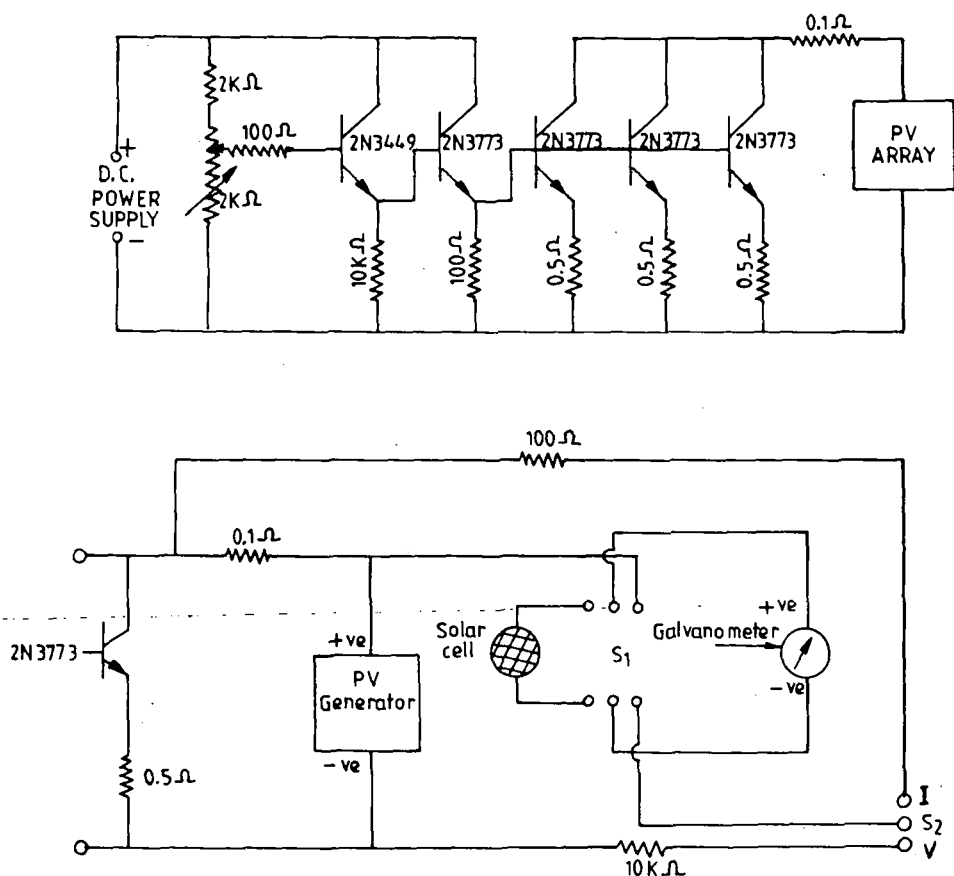


Fig. 3. Circuit of current/voltage plotter for solar cells and array.

reference solar cell is disconnected by using S1 and either current (in terms of voltage drop across a series resistance of 0.1 ohm) or voltage is measured by using switch S2 to either I or V position respectively. Using a resistance of 100 ohm in series with the galvanometer, the current for measurement is 1/1000 of the current flowing through 0.1 ohm resistance. Thus, the maximum current that can be used is 10 amps. Similarly, using a 10 kilo-ohm resistance for the voltage measurement, the maximum voltage that can be measured is 100 volts.

To obtain the I-V plot on an X-Y recorder, the voltage across the 0.1 ohm resistance and the PV device (with +ve terminals as common) are provided at the output terminals. Thus, I-V characteristics can be plotted independent of the galvanometric measurement. A six volts (100 mA) source is required to drive the current-voltage characteristics meter. Input power can be supplied by a 6 volts constant voltage source, such as a battery or a DC power supply. It can also be operated by a separate photovoltaic power supply which may not be a constant 6 volts source. The other advantage of this meter is that it can also be operated by self-biasing from the same solar module or same array which is under test.

### Battery

In our experimental facility 20 (Exide) batteries are connected in different configurations to provide the power for different pump and DC/AC inverter. These batteries are charged by the power of the PV generator. The specifications of each battery are the rated voltage of 6 volts and current storage capacity of 180 amps.

These batteries are normally used to store electrical energy and act as a constant DC voltage regulator. The battery voltage is to be fixed according to the  $V_m$  of a PV array (for a particular configuration of PV modules) which is almost constant above a solar insolation of 400 W/m<sup>2</sup> and the motor terminal voltage at maximum motor pump efficiency or input voltage of inverter. In this case batteries and PV modules are configured in such a fashion that the load current of a motor or inverter at its maximum efficiency point can be supplied from the battery bank and simultaneously batteries can be charged near the  $I_m$  region of this PV array under fluctuating solar insolation levels.

Poor efficiency, heavy maintenance, and short life are the major drawbacks in using the batteries for this application. Another drawback of using a battery bank in a pumping application is that a high induced voltage in the excitor circuit damages the rectified elements and the motor field winding at the time of starting a brushless motor.

### DC-AC Inverter

The solid state based 1KVA (APLAB) DC-AC inverter has been connected in the experimental facility through a battery or directly with the PV generator, as shown in Fig. 2. The inverter produces nearly sine wave of frequency 50 Hz at 220 volts AC by intaking of 110 volts DC power supply. The efficiency of the inverter is 85% at full load condition. The inverter has its own protection devices to protect it from the short circuit condition, i.e., a reverse input terminal and high and low input voltages.

The DC-AC inverter produces AC power from a DC source (PV generator) and it is required for running an AC motor. The main problem of connecting an inverter in this application is that the inverter cannot run when it is directly powered by the PV array. This is due to fluctuation of the input voltages with variations of solar insolation levels in the field. Therefore, a battery bank

or electronic control device is required which decreases the total system efficiency. Another problem is that the inverter is tripped by passing a high current at the time of starting the motor.

### MPPT (DC-DC Converter)

One 600 watts MPPT (60V and 10A) is connected to our testing facility, which is designed and developed by CNRS (France). It is operated by a 220 volts AC supply.

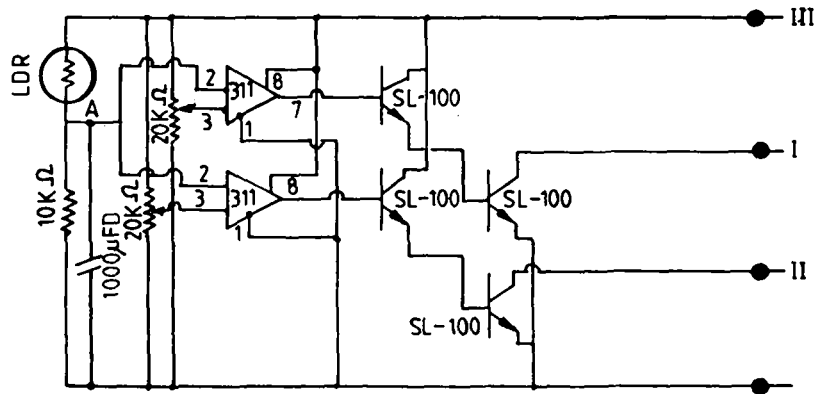
The matching of the load to the solar cell array is accomplished by incorporating an electronic control device – an MPPT for maximum utilization of PV energy into the system. The MPPT may be viewed as a time variable transformer (TVT), in which the transformation ratio is changed electronically, corresponding to the variations of the load operating point due to the variations of the insulations. The basic principle of an MPPT is that it forces the pump to track electronically the maximum power of a PV array at the given load. It is reported [4] that a single stage centrifugal pump, for an application of a static water head of less than 10 metres, connected with a DC motor, can be designed in such a way that it can track near the maximum power point of the PV array output from morning to evening without an MPPT. However, a multistage centrifugal pump or a positive displacement pump, for a static water head of more than 10 metres, connected to a DC motor cannot track the maximum power of a PV array for a whole day without an MPPT.

### Switching Device

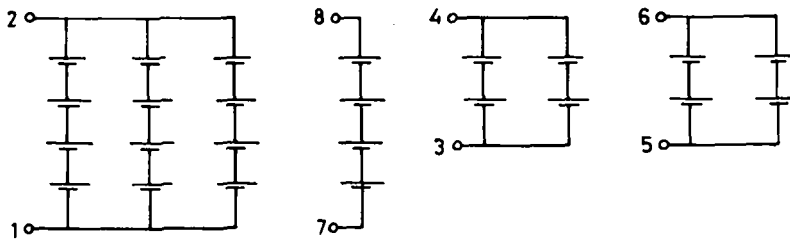
The electrical coupling efficiency of a photovoltaic water pump system increases [5,6] by using an appropriate combination of PV modules in accordance with the variation of solar insolation levels. If the number of modules connected in parallel is increased at a low solar insolation level by reducing the number of modules connected in series (where the total number of modules is fixed), the field performance efficiency of the direct coupled pump is improved. An automatic control electronic circuit, as shown in Fig. 4, for changing the combinations of PV modules has been designed and fabricated and consists of:

- i) a sensing circuit,
- ii) a comparator circuit, and
- iii) a switching circuit.

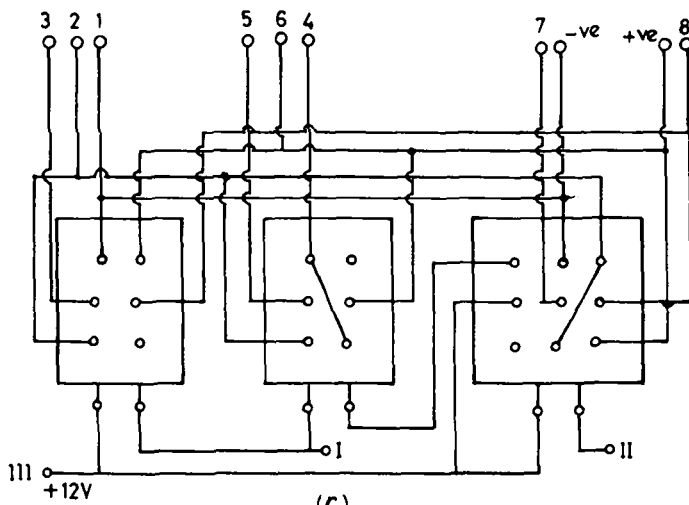
The sensing circuit senses solar insolation by the LDR or short circuit current of a PV device. The resistance of the LDR varies with solar insolation levels. This LDR is connected in series with another resistance (10 k) across a 12 volts DC source. The voltage of the junction point (A) between the resistance and the LDR varies with solar insolation levels in the field and it sensed in terms of voltage to pin No.2 of two ICs (311). This sensing signal is compared with a reference signal which is equivalent to the 'cut-off solar insolation' of a particular pump in a comparator circuit, as discussed by Koner et al. [7]. Two potentiometers (20 k) are used across the same 12 volts DC supply for producing fixed reference voltage for the two ICs. These reference voltages are supplied to pin No.3 of these ICs. A voltage equal to that developed at point A for a particular solar insolation can be generated for the ICs' reference voltage by controlling the potentiometer. By this process, the reference voltage can be changed for different pumping systems according to their 'cut-off solar insulations'.



(a)



(b)



(c)

Fig. 4. Automatic switching controller circuits for changing the pattern of combining the PV modules  
 a) Sensing and comparator circuit.  
 b) Connecting patterns of the terminals of PV modules.  
 c) Relay circuit.

Three combination patterns of PV modules can be obtained by this facility. At very low solar insolation, two ICs and three relays are at 'OFF' condition. At that time, for a particular arrangement of the terminals of the PV modules, it would give a particular configuration. IC-1 will be 'ON' and IC-2 will be 'OFF' at medium solar insolation. Because of the 'ON' condition of IC-1, the first two relays will operate and change the configuration for a second set. When the solar insolation is high, both the ICs will turn 'ON'. The relay drive circuit is configured in such a fashion that when both ICs are at 'ON' condition, only relays 1 and 3 will operate and it will give the third type of combination of PV modules.

Each relay draws a current of 250 mA which cannot pass through any IC. Therefore, a buffer circuit has been connected in between the ICs and the relays, which comprises two SL-100 transistors. The solar insolation varies very rapidly in the field which generates a highly fluctuating voltage at point A. To stabilize this fluctuation, one 1000 mfd capacitor is connected between point A and the ground.

### Motor

In this experimental facility, two types of AC and DC motors can be characterized by measuring their terminal voltage, intake current, total resistance of field and coil and speed of the motor. A DC motor directly connected to a PV generator is cheaper and it simplifies the system design as compared to the use of an AC motor for a stand alone PV system. DC motors can be classified into three categories according to their mechanism as: i) series, ii) shunt and iii) separately excited. Among these motors the DC series motor has been chosen as a specific example in this study. A DC series motor can be characterized as

$$V_t = I_a R_t + E_a \quad (2)$$

$$E_a = M I_a \omega \quad (3)$$

$$T = M (I_a)^2 \quad (4)$$

$$E_m = P_{out}/P_{in} = \omega^m T^m / (V_t I_a) \quad (5)$$

### Pump

Pumps are also divided into two categories according to their working mechanism: i) Rotodynamics and ii) Displacement. Both type of pumps can be characterized in the present facility by the measurement of the speed, water head and flow of a pump. The rotodynamics pump is a ventilator load torque pump which can be matched to a PV generator without power conditioning for a static water head of less than 10 metres. The centrifugal pump was chosen for verifying the performance of the test system. A centrifugal pump can be mathematically characterized as

$$h = K_{p1} (\omega^p)^2 \quad (6)$$

$$Q = K_{p2} \omega^p \quad (7)$$

$$E_p = g Q h / (\omega^p T^p) \quad (8)$$



## OTHER OPTIONS OF THE TESTING FACILITY

Apart from the technical studies of the PV water pump system, the testing facility has the option of measuring the operating norms, average daily efficiency and the cost analysis of the system as discussed below.

### Operating Norms

The operating norms to design a PV water pump are: i) current, ii) voltage of the motor-pump at its maximum efficiency point and its threshold condition, and iii) threshold solar insolation for a particular load. The required threshold solar insolation not only depends on the starting voltage and current, it also depends on the series and parallel combination of PV modules. The threshold solar insolation can be reduced by changing the combination of the PV modules.

### Average Daily Efficiency

The average daily efficiency ( $E_{mp}^d$ ) of PV water pump system is defined as

$$E_{mp}^d = \frac{\text{total water discharged in one day (watts)} \times 100}{\text{solar insolation in one day} \times \text{area of the PV array (watts)}} \quad (9)$$

The average daily efficiency can be maximized by either increasing the individual component efficiency or by reducing the operating norms of the PV water pump or both.

### Projected Specific Capital Cost

Projected specific capital cost (SCC) is not an economic analysis of a system. It can give a preliminary idea about the cost of a system only. It is defined [4] as

$$SCC = C/(p g h V_w) \text{ Rs./KJD} \quad (10)$$

## FIELD PERFORMANCE OF THE TESTING FACILITY

To verify its field performance we have measured an array comprising of 5 series and 4 parallel C.E.L. PV modules. Figure 5 shows the I-V plot of a C.E.L. (Central Electronics Ltd., Sahibabad, India) PV module using an X-Y plotter and galvanometer. The two curves are nearly identical. The slight difference in current values is due to the resistance value not being exactly equal to the calibrated value. This difference can be eliminated by using precision resistances. The photovoltaic parameters using plotter are comparable to the values measured using a maximum power point tracker (which is available in our laboratory). Table 2 shows a comparison of the values.

This meter has the advantage that it can operate by self-biasing. Therefore, an I-V plot of a C.E.L. PV module has been made by using a constant 6 volts input and direct input power supply from a PV module which is under test, as shown in Fig. 6. The I-V curve of one PV module is

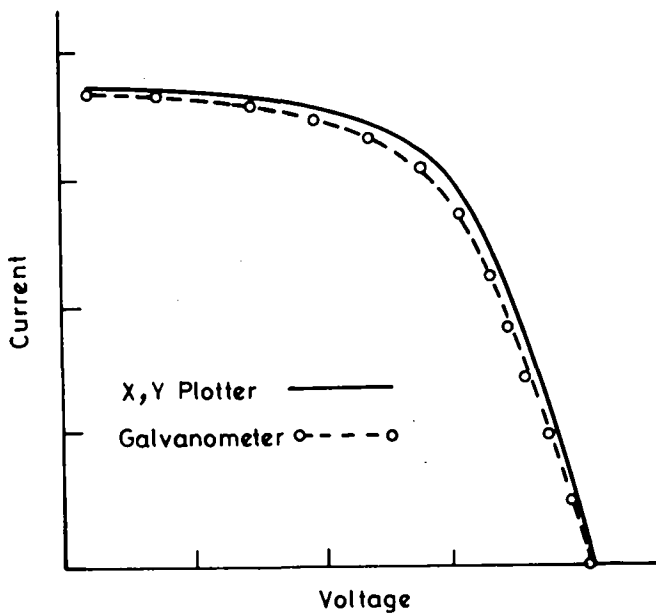


Fig. 5. Measurement of I-V performance of a r-v module by galvanometer and X-Y recorder.

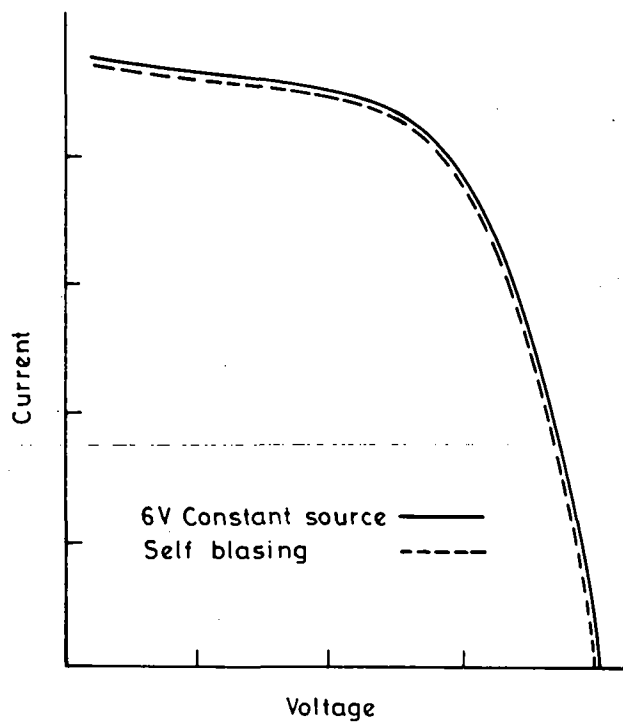


Fig. 6. Comparison of I-V performance for self-biasing and constant 6 volts source.

found to be shifted from that which is obtained when the plotter is supplied from an independent 6 volts source. This little shift is, however, negligible( less than 1% of  $I_{sc}$ ). Therefore, measurement under self-biasing can be done avoiding use of any other source without affecting the current values.

The performance of the automatic control switching has been checked by the experimental study of a pump (C.E.L.) in the field. The improved daily average efficiency of the pump using the switching device and the accuracy of the solar insolation level for switching are shown in Fig. 7.

**Table 2. Comparative performance between present plotter and MPPT at solar insolation 970 W/m<sup>2</sup> and ambient temperature 32°C.**

Configuration of PV Modules	Present Plotter			MPPT		
	$V_{oc}$	$I_{sc}$	$P_m$	$V_{oc}$	$I_{sc}$	$P_m$
1s x 1p	18.0	1.9	17.9	18.0	2.0	18.2
2s x 2p	35.8	3.9	71.8	36.0	4.0	72.5
5s x 4p	72.0	8.0	391	not possible		

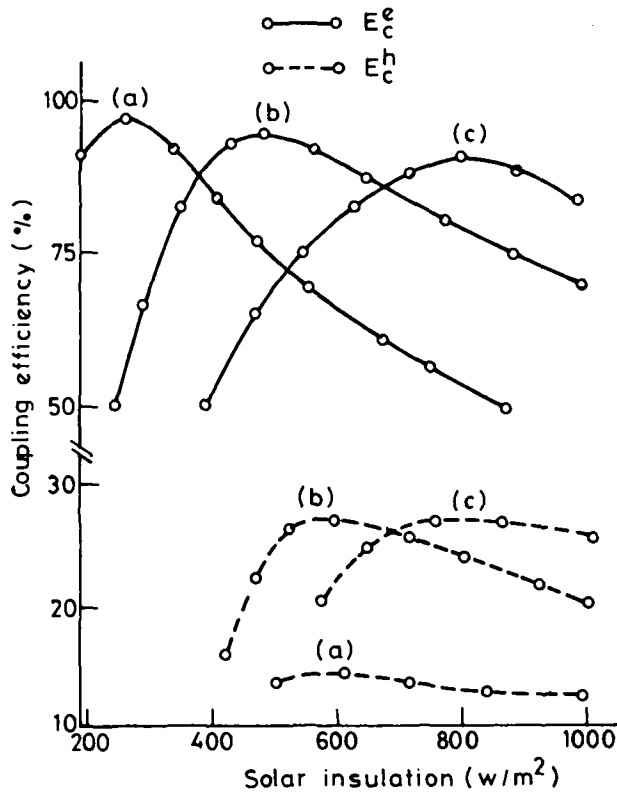


**Fig. 7. Variations of different coupling efficiencies of C.E.L. photovoltaic water pump system with solar insulations under different combinations of PV modules:**  
 a) 4 series x 6 parallel;      b) 6 series x 4 parallel; and      c) 8 series x 3 parallel.

## FIELD PERFORMANCE OF PUMP

The testing facility has been used to conduct a comparative field study of two different systems, using a series DC motor-pump (C.E.L., India) and a brushless DC motor-pump (K.S.B., AQUASAL 50M, Germany), the specifications of which are given in Table 3.

The C.E.L. pump is characterized by a standard DC power supply as shown in Fig. 8. The K.S.B. pump is characterized by using different combinations of PV modules at different times of day as shown in Fig. 9. The reason for doing so is that the K.S.B. pump system has a brushless DC motor which cannot be directly connected to a battery bank or a constant voltage source. From these studies and the field condition  $V_m$  and  $I_m$  data of the PV array as measured by an I-V plotter, the requirement of the optimum number of PV modules connected in series and in parallel has been found. It is observed that (i) three strings of PV modules (C.E.L.) in parallel, each comprising seven PV modules in series and (ii) four parallel strings each with five PV-modules in series are required to get the optimum efficiency for the C.E.L. and K.S.B. pumps, respectively.

The power intake of a motor pump in terms of operating voltage and current, maximum power of a PV generator, flow rate, speed, threshold conditions of a PV water pump and water discharge for a standard day of both systems, have been collected from field study, where water head and solar insolation are variables. The motor-pump efficiency and coupling efficiency have been calculated and the variation of those for both the systems with solar insolation are shown in Figs. 7-9. The motor-pump efficiency, daily average efficiency and SCC have also been calculated from these data for different water heads. A comparative study of both systems is shown in Table 4. They could not be compared at the same water head because the C.E.L. pump efficiency is maximum at 10 metres whereas the K.S.B. pump efficiency is maximum at 6 metres static water head. The reported [4] projected SCC of K.S.B. pump is \$1.5 /KJD at a static water head of 6 metres which is comparable with that of the present study.

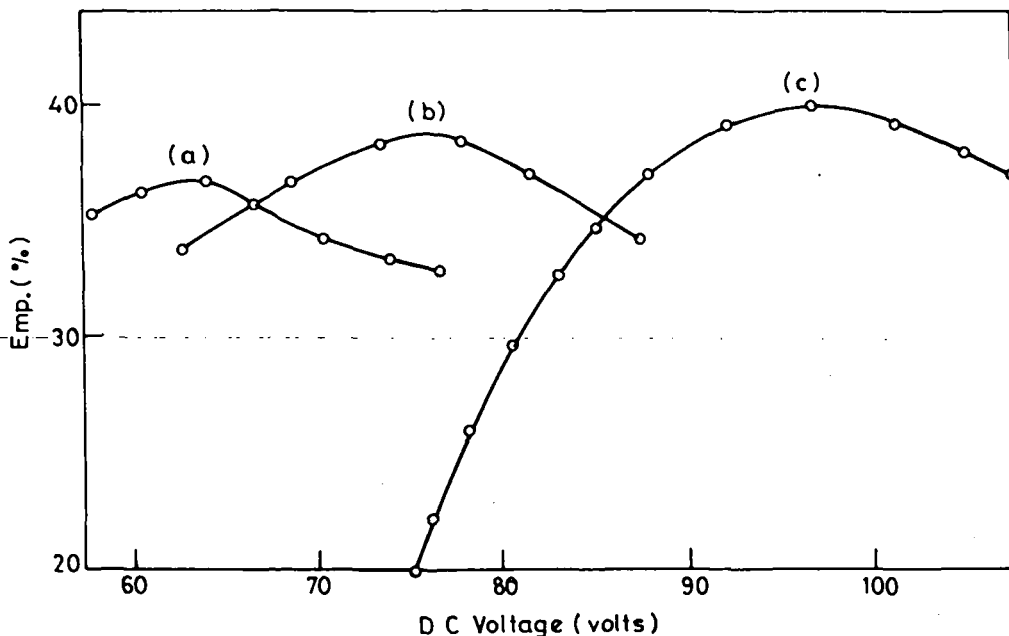


Fig. 8. The motor-pump efficiency of C.E.L. pump system versus motor terminal voltage for the water head of: a) 5 metres; b) 7 metres; and c) 10 metres.

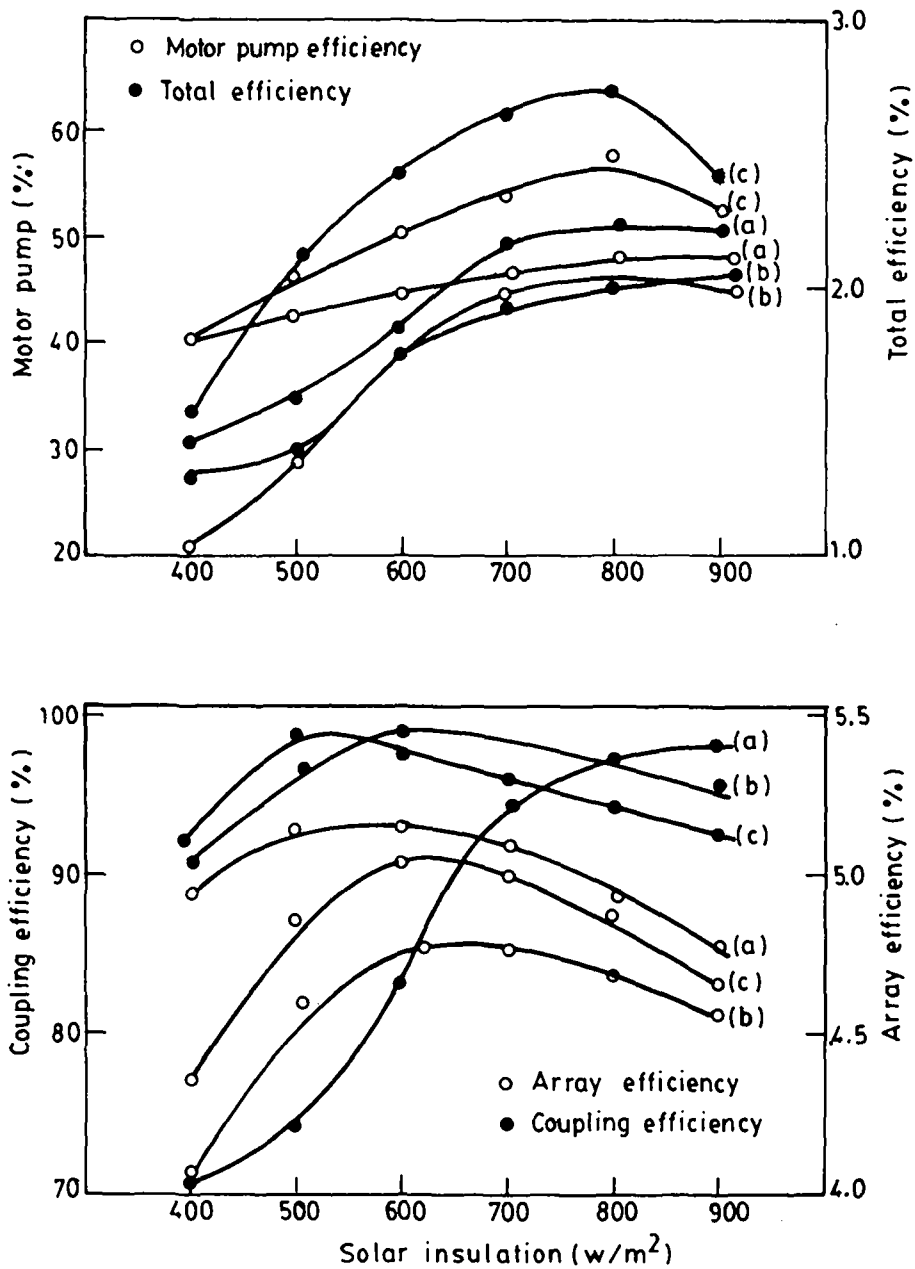


Fig. 9. Array efficiency and different efficiencies of K.S.B. pump versus solar insolation for the combination of PV-modules:  
 a) 5 series x 3 parallel;      b) 5 series x 4 parallel; and      c) 4 series x 4 parallel.

**Table 3. Specifications of water pump systems.**

Description of Pump	Rated voltage (volts)	Rated wattage (watts)	Water head up to (m)
C.E.L. DC series motor and centrifugal pump	60	300	6
K.S.B. brushless DC motor and centrifugal pump	68	480	11.5

**Table 4. Comparison of the field performances of C.E.L. and K.S.B. photovoltaic water pump systems.**

Characteristics	C.E.L. water pump	K.S.B. water pump
$(E_{mp})_{peak}$	40% at WH = 10 m 39% at WH = 7 m 37% at WH = 5 m	47% at WH = 8 m 58% at WH = 6 m 52% at WH = 5 m
Total water discharge for a standard day (6 kWh/day)	26m at WH = 10 m 38m at WH = 7 m	48m at WH = 7 m 58m at WH = 5 m
Capital cost	Rs. 52000.00	Rs. 67000.00
Threshold condition:	at WH = 7 m	at WH = 6 m
Voltage	63 volts	45 volts
Current	2.3 amps	3.1 amps
Solar insolation	400 W/m <sup>2</sup>	380 W/m <sup>2</sup>
Average daily efficiency	1.34% at WH = 10 m 1.35% at WH = 7 m	1.90% at WH = 6 m 1.68% at WH = 5 m
Projected SCC (Rs./KJD)	20.4 at WH = 10 m 20.0 at WH = 7 m	20.3 at WH = 6 m 23.1 at WH = 5 m

**CALCULATION PROCEDURE**

The different efficiencies of a PV-water pump system are the PV array efficiency ( $E_a$ ), motor-pump efficiency ( $E_{mp}$ ), power conditioner efficiency ( $E_{pc}$ ), electrical coupling efficiency ( $E_c^e$ ), hydraulic coupling efficiency ( $E_c^h$ ) and the total system efficiency ( $E$ ). The array efficiency has already been defined in equation (1). The motor and pump efficiencies can be separately evaluated using equations (5) and (8) by an indirect process for mono-block motor-pump systems. However, the motor-pump efficiency has been directly evaluated by the following equation

$$E_{mp} = g Q h / (V_t I_a) \tag{11}$$

Other efficiencies can be computed by the following equations

$$E_{pc} = V_t I_a / (V_m I_m) \tag{12}$$

$$E_c^e = V_t I_a / (V_m I_m) \tag{13}$$

$$E_c^h = g Q h / (V_t I_a) \tag{14}$$

$$E_t = E_a \times (E_{pc} \text{ or } E_c^e) \times E_{mp} \tag{15}$$

**OBSERVATIONS AND DISCUSSIONS**

As shown in Fig. 9a, the array efficiency varies with solar insolation levels, which is explained by the variation of series resistance effect of the solar cell. The series resistance of a solar cell decreases with the increase of solar insolation because of the decreased sheet resistance of PV material. Therefore, the increase of array efficiency with increased solar insolation has thus been found in the first portion of the Fig. 9a for any combinations of PV modules. Another factor which affects the array efficiency is the temperature. At higher solar insolation levels, the array efficiency is reduced because the temperature effect is dominant as compared to the sheet resistance effect of the solar cell in this portion. Another source of variation of array efficiency which depends on the combination of PV modules is due to the effect of self-shadowing from the front contact grid of a single crystalline solar cell module [8].

Wide deviations of field measured values of  $V_m$  and  $I_m$  of the PV array from quoted values have been found. The cause of the variations is due to the involvement of a large number of environmental factors as discussed and modelled in Ref. [9].

The reported highest water heads of C.E.L. and K.S.B. pumps are 6 and 11.5 metres respectively. The K.S.B. pump cannot raise the water head more than 10 metres whereas the C.E.L. pump can easily raise the water head up to 10 metres with higher efficiency. The efficiency of the C.E.L. pump increases with increasing water head, but the K.S.B. pump efficiency increases to some extent with fixed value of water head but then it decreases with increasing water head as shown in Table 4. A discussion of these effects due to the design of the pump is reported in Ref. [10].

An electronic controller for changing the configuration of PV modules has been tested in the field to improve the daily average efficiency of the C.E.L. pump. Using this instrument the variations of coupling efficiencies of the C.E.L. pump with different combinations of PV modules,

at various solar insolation levels, are shown in Fig. 7. At least three combinations are required to get an optimum match between the pump and the PV generator for the solar insolation levels from  $200 \text{ W/m}^2$  to  $1000 \text{ W/m}^2$  [5,6]. However, in this study, it was found that two combinations are sufficient to get the optimum hydraulic efficiency as shown in Fig. 7. The third combination is not required because in this combination electrical coupling efficiency is improved whereas the hydraulic efficiency reduces drastically due to the under voltage of the motor.

## CONCLUSIONS

A multipurpose photovoltaic water pump testing system has been successfully designed and fabricated. The testing system has been used to undertake a comparative study of two different pump sets in the field. From this comparison study it can be observed that the C.E.L. PV water pump is a better choice than the K.S.B. pump system under Indian conditions for the following reasons:

- i) the C.E.L. pump is available 'off the shelf' in the Indian market;
- ii) even though the efficiency of the C.E.L. subsystem is lower, the SCC is comparable to that of the K.S.B.; and
- iii) the C.E.L. subsystem efficiency is affected less by a change of water head and solar insolation compared to the K.S.B. subsystem.

## NOMENCLATURE

$SI$	= Solar insolation, $\text{W/m}^2$
$STC$	= Standard test condition
$A$	= Area of PV array, $\text{m}^2$
$MPPT$	= Maximum power point tracker
$V_m$	= Voltage at maximum power point of a PV array, volts
$I_m$	= Current at maximum power point of a PV array, amps
$I_{sc}$	= Short circuit current of a PV array, amps
$V_{oc}$	= Open circuit voltage of the PV array, volts
$I_B$	= Base current of transistor, amps
$I_a$	= Armature current of the motor, amps
$V_t$	= Motor terminal voltage, volts
$R_t$	= Total resistance of armature and field coil, ohm
$\omega^m$	= Speed of the motor, rad/s
$\omega^p$	= Speed of the pump, rad/s
$T^m$	= Torque of the motor, Nm
$T^p$	= Torque of the pump, Nm
$M$	= Motor constant, $\text{Nm/A}^2$
$E_m$	= Motor efficiency, %
$E_p$	= Pump efficiency, %
$Q$	= Flow rate, l/s
$C$	= Capital cost of a PV-water pump system, Rs.
$\rho$	= Density of water, $\text{kg/cm}^3$



- $g$  = Gravitational acceleration  $m/s^2$   
 $h$  = Static water head, m  
 $V_w$  = Total volume of water pumped per standard day,  $m^3$   
 $K_{p1}$  and  $K_{p2}$  are the pump constants,

## REFERENCES

1. Hermann, B., H. Karl, E. Kopf and G. Lehner (1986), Realistic Indoor Testing of Photovoltaic Water Pumping System, *Solar Energy*, Vol.38, No.4, pp.275-279.
2. Pulfery, D.L., P.R.B. Ward and W.G. Dunford (1987), A Photovoltaic Powered System for Medium Head Pumping, *Solar Energy*, Vol.38, No.4, pp.255-256.
3. Chandratilleke, T.T. and J.C. Ho (1986), A Study of a Photovoltaic Array for Water Pumping, *Solar & Wind Technology*, Vol.3, No.3, pp.59-71.
4. Report of the UNDP Project GLO/80/003 (1983), Sir William Halcrow and Partners in association with Intermediate Technology Power Ltd.
5. Faldella, E. (1989), *Matching and Control Technique for Optimizing Automatic Management of Photovoltaic Pumping Systems*, presented at the Workshop on Materials Science and Physics of Non-conventional Energy Sources, Trieste, Italy.
6. Salameh, Z. and C. Liang (1990), Optimum Switching Points for Array Reconfiguration Controller, *Proc. of 21st IEEE Photovoltaic Specialists Conf.*, pp.971-976.
7. Koner., P.K., J.C. Joshi and K.L. Chopra (1991), *Study of a Pumping load by Different Configurations of Photovoltaic Modules*, paper presented at ISES Solar World Congress-1991, Denver, Colorado, U.S.A.
8. Koner, P.K., V. Dutta and K.L. Chopra (1992), *Grid Shadowing Effect on Field Performance of cz-Si Solar Cells and Array*, Accepted for Presentation at ASME International Solar Energy Conference, to be held at Hyatt Regency, Maui, Hawaii, April 4-8, 1992.
9. Koner, P.K., J.C. Joshi and K.L. Chopra (1991), Quantitative Field Performance Analysis of Photovoltaic Array, *International Journal of Energy Research*, Vol.15, No.6, pp.473-482.
10. Koner., P.K., J.C. Joshi, A.K. Mukerjee and K.L. Chopra (1991), Analysis of Optimum Matching of a D.C. Series Motor Driven Centrifugal pump to a Photovoltaic generator, *International Journal of Renewable Energy*, in press.